



Titanium and Fluoride Co-substitution in Hydroxyl Apatite

F. Asjadi, E. Salahi*, I. Mobasherpour

Department of Ceramic, Materials and Energy Research Center, Karaj, Iran

PAPER INFO

Paper history:

Received 22 February 2015

Accepted in revised form 18 April 2015

Keywords:

Ti containing hydroxyl apatite

Fluorohydroxy apatite

Surface charges

Nano structures

ABSTRACT

Titanium and fluoride-containing hydroxyl apatite were synthesized through precipitation method following by a hydrothermal stage at 100°C for 6 hours. XRD analysis of the sample calcined at 650°C for 1 hour revealed that all samples have pure apatite structure. The existence of Fluoride substitution in apatite structure was confirmed by FTIR (Fourier Transform Infrared Spectroscopy) analysis. Surfaces of the samples were studied by zeta potential measurements. Investigating cell parameter and also FWHM (Full Width at Half Maximum) of phosphate ν_1 peak in Raman spectra showed some different behaviour in samples with titanium and high fluoride concentration attributed to different position of titanium in these samples. Scanning electron microscopy (SEM) was used for investigating the morphology of samples. The Morphology of particles was not affected by adding titanium and fluoride.

1. INTRODUCTION

Papers body must be Times New Roman 10 in two columns and line space during whole paper is 1 cm.

Also, normal paper size for ACERP is 6-8 journal pages. If any paper exceeded more than 10 journal pages, we will take off from production; never publish it! Unless another reduce the size of the manuscript.

Because of apatite structures, extensive substitutions are possible in all atomic sites. Some of them can be produced in synthesize stage and others by ion exchange among solid apatite and solutions. Calcium sites can be occupied in some extent by monovalent ($\text{Ag}^+_{[1]}$), divalent ($\text{Fe}^{2+}_{[2]}$ and $\text{Sr}^{2+}_{[3]}$), trivalent ($\text{Ce}^{3+}_{[4]}$) anions while $\text{VO}_4^{3-}_{[5, 6]}$, $\text{AsO}_4^{3-}_{[7]}$, $\text{SiO}_4^{4-}_{[8, 9]}$, $\text{SO}_4^{2-}_{[10]}$ and $\text{CO}_3^{2-}_{[11]}$ can be located at phosphate positions, but the latter are also found in OH positions. The apatite will incorporate half of the elements in periodic table [12]. Titanium incorporation in apatite structure was studied by different researchers [13-15]. Although the position of titanium in apatite is controversial, the possibility of the incorporation of titanium in apatite structures accepted by all researchers [13, 16-19]. Wakamura introduced Ti substituted hydroxyl apatite as a photo catalyst [20-22]. It is also reported that TiHAp has potential to be used as an alternative bioactive coating on metallic prostheses,

dental and orthopaedic applications and bioactive scaffolds [23]. On the other hand, fluorohydroxyl apatite is another promising biomaterial due to dissolution-resistant property and comparable biocompatibility to hydroxyl apatite. Considering these studies, it seems that cosubstitution of these ions could have an interesting characteristics to be used in different applications. The most common methods to synthesize substituted hydroxyl apatite are coprecipitation and ion exchange methods. Sugiyama [18] used both coprecipitation and ion exchange methods to synthesize TiHAp. Huang [23] and Ergun [14] also studied synthetic TiHAp by using tetraethylorthotitanate as titanium source. There are numerous researches about the role of titanium in hydroxyl apatite and many researches about the fluoridated hydroxyl apatite, though the effects of both ions are hardly reported [24]. This compound could have been used in environmental era as adsorbent or photo catalyst to remove pollutants. Although it is required more investigations and researches, it could also use as a biomaterial.

The purpose of this work is to use coprecipitation method followed by hydrothermal stage to synthesize titanium and fluoride substituted hydroxyl apatite and characterize influences of these substitutions on each other and also on hydroxyl apatite properties.

2. EXPERIMENTAL PROCEDURES

2.1. Synthesize route

Since Titanium salts are hydrolysed instantly in aqueous solutions, titanium

*Corresponding Author's Email: esmaeil.salahi@outlook.com (E. Salahi)

isoporpoxide (Aldrich, Germany, 20527) and triethanolamine (Sigma- Aldrich, Germany, 90279) were mixed in the molar ratio of 2:1 to form hydrolysis resistant complex [25] and this complex was used as a source of titanium. Titanium-containing HAp (denoted as TiHAp in the following) $X_{Ti}=(Ti+P)/P=0.05$ were synthesized by coprecipitation method based on reaction between calcium nitrate(Sigma- Aldrich, Germany, 237124) and di ammonium hydrogen phosphate(Merck, Germany, 101207). Ti Complex and Calcium solution were added gutty to phosphorus solution under continuous stirring while the temperature was maintained at $50\pm 2^\circ\text{C}$. The amount of Ca+Ti and P were 0.1 and 0.06 mole respectively, so the ratio $Ca/(P+Ti)=1.67$ was satisfiable. pH was adjusted to 10 by adding ammonia solution. The TiHAp gel was aged for 6 hours at 100°C . The products were filtered, washed several time with ethanol and water then dried at 70°C for 24 hours and eventually milled.

The obtained powder was calcined at 650°C for 1 hour (with heating rate of $5^\circ\text{C}/\text{min}$). The fluoride-containing samples were synthesized by mentioned processes and by adding fluoride solution to primary solution. The amount of fluoride adjusted in order to fill 0.25 and 0.75 of hydroxyl positions and these samples were denoted as TiHApF0.25 and TiHApF0.75, respectively.

2.2. Characterisation Powder X-ray diffraction method was carried out with a Philips diffractometer (PW 3710), Cu K_α radiation, in the 2θ range of $25-45^\circ$. In order to have an accurate studies of peaks positions, the measurements carried out by step size of 0.0005° and step time of 1 second at room temperature.

Ramanspectroscopy measurements were performed by using the 532 nm line of a linearly polarized He-Ne laser, equipped with an Olympus microscope with $\times 10$, $\times 50$, $\times 100$ and $\times 150$ objectives, a motorized x-y stage and auto-focus. Laser power was controlled by means of a series of density filters. The position, FWHM and other parameters of peaks in X-ray diffraction and Raman patterns were then determined by fitting with Voigt functions using the Fityc software[26], after linear background removal. Cell parameters were obtained by Unit cell program[27]. FTIR measurements were carried out by using Perkin-Elmer (Spectrum 400) in the wave number range of $450-4000\text{cm}^{-1}$.

Zeta potentials of the samples were measured by Zeta sizer, Malven Enstrumetn Ltd. Each suspension ejected twice and measurements were carried out three times for every injected sample and the average of six measurements is reported here.

3. RESULT AND DISCUSSION

XRD patterns of the pure hydroxyl apatite, TiHAp, TiHApF0.25 and TiHApF0.75 are reported in Figure 1.

All peaks are assigned to the single hydroxyl apatite phase (JCPDS86-0740). No remarkable differences are observed in the XRD patterns of the samples by introducing Titanium and fluoride, It indicated that the apatite crystal lattice is not affected by the presence of Titanium and fluoride.

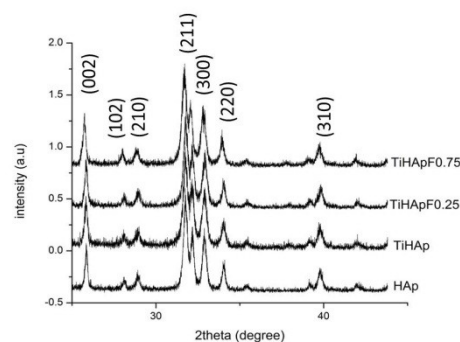


Figure 1. XRD Patterns of the samples, HAp, CaTi, CaTiF0.25, CaTiF0.75.

Figure 2(a). shows FTIR spectra of the samples calcined at 65°C . Figure 2(b). shows the extended region of wave number $3400-3700\text{cm}^{-1}$ of the same spectra. The bands at 3571 and 631cm^{-1} corresponded to the stretching and vibration modes of hydroxyl groups, respectively. Intense bands at 1085 , 1014 and 961cm^{-1} are corresponded to P-O stretching vibration modes and two peaks at 593 and 572cm^{-1} are attributed to O-P-O bending mode. TiHAp shows no peaks other than hydroxyl apatite peaks. By introducing Titanium the intensity of hydroxyl peak decreases but no other particular difference was observed in FTIR spectrum. Decreasing the OH intensity is caused by decreasing the crystallinity of the sample. Moreover, Since the phosphate groups have three negative charges which is more negative compare to titanium tetrahedrals with four negative charges, decreasing the OH intensity is also occurred by releasing the OH groups for maintaining the charge balance in case of the replacement of Titanium in phosphate position.

Splitting and shifting of the OH peak at 3570cm^{-1} is observed in fluoridated hydroxyl apatite indicative of F^- substitution in OH positions. By increasing the fluoride concentration the intensity of the new peak at $\sim 3548\text{cm}^{-1}$ increased. This new peaks arise from OH...F bond.

The XRD and FTIR results proved that titanium and fluoride placed in hydroxyl apatite structure. There are some very low intensity peaks at the wave number about 3600cm^{-1} in FTIR spectrum of CaTiF0.75 Figure 2(b). This bands were reported to form due to increasing the surface binding of the ions with hydroxyl ions, for instance the surface P-OH binds which formed with protonation of the surface [22] or Ti-OH surface binds[15].

Raman spectra of the samples calcined at temperature 650°C in the frequency region $100-1400\text{cm}^{-1}$ were

reported in Figure 3. The extended image of the phosphate ν_1 peak is also showed in this figure.

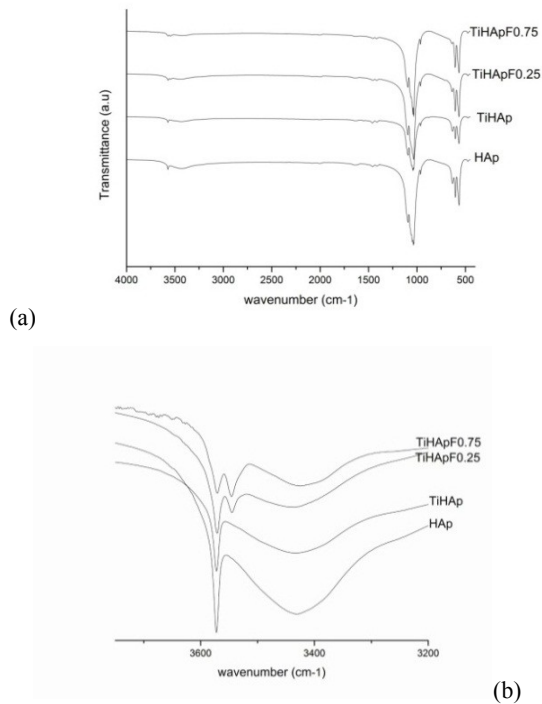


Figure 2. FTIR spectra of the samples calcined at 600°C a: Wavenumber of 400-4000 and b: extended image of the selected part.

All Samples showed the pure apatite structure. In pure apatite, the 1076 cm^{-1} , 1052 cm^{-1} , 1047 cm^{-1} , 1040 cm^{-1} (sh), and 1028.5 cm^{-1} bands arise from $\nu_3\text{ PO}_4^{3-}$, the very strong 962 cm^{-1} band are attributed to $\nu_1\text{ PO}_4^{3-}$, the 614 cm^{-1} , 607 cm^{-1} , 590 cm^{-1} , and 579 cm^{-1} bands are associated to $\nu_4\text{ PO}_4^{3-}$, and the 447 cm^{-1} and 431 cm^{-1} bands corresponded to $\nu_2\text{ PO}_4^{3-}$. The groups of weak intensity bands in the 50 cm^{-1} to 329 cm^{-1} region derive from translations of the Ca^{2+} , PO_4^{3-} and OH^- ions and liberations of the PO_4^{3-} ions. The 329 cm^{-1} are assigned to vibrations of the $2[(\text{CaII})_3(\text{OH})]$ sub lattice of hexagonal HAp, and the band at 285 cm^{-1} primarily to libratory phosphate motions[28].

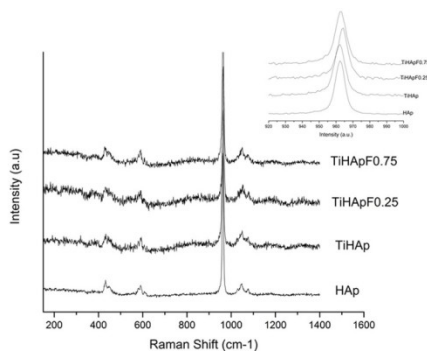


Figure 3. Raman spectra of HAp, TiHAp, TiHAp0.25 and TiHAp0.75 samples. Phosphate ν_1 peak of the samples were shown in a small picture at right above of the figure.

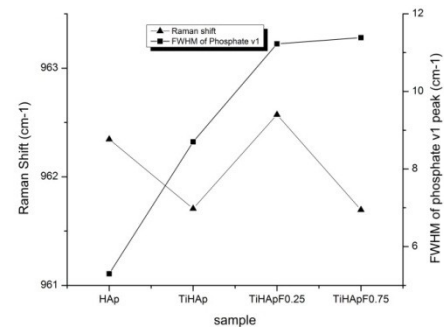


Figure 4. Position and FWHM of phosphate ν_1 peaks in Raman spectra of HAp, TiHAp, TiHAp0.25 and TiHAp0.75 samples.

By adding Titanium and fluoride no new peak was observed in Raman spectra but the position and FWHM of the phosphate peak changed. The results of the fitting processes were shown in Figure 4. Adding titanium into Hap led to broadening of the phosphate peaks in Raman spectrum and also shifting the position of the peaks toward lower wave number. Broadening and shifting of the Raman peaks was due to disorder structure and microscopic strain in the structure. In TiHAPF0.25 and TiHAPF0.75 the FWHM of the phosphate peak increased, however in latter sample the increase wasn't remarkable. In TiHAPF0.25 sample, the phosphate ν_1 peak at $\sim 961\text{ cm}^{-1}$ shifted to higher, but in TiHAPF0.75 it shifted to lower Raman shift which is not supported by effects of fluoride substitution in hydroxyl apatite on Raman spectrum which is reported by other authors indicating the blue shift of the phosphate ν_1 peak in Raman spectrum[29].

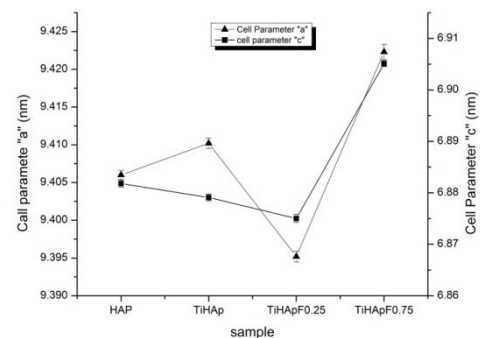


Figure 5. Cell parameters of HAp, TiHAp, TiHAp0.25 and TiHAp0.75 samples.

Figure 5. shows cell parameters of different samples. It shows increasing of the "a" parameter and decreasing of the "c" parameter for TiHAp sample and inverse behaviour in TiHApF0.25. In this sample replacing of F decreases the cell parameter. As it is reported by many authors, the inverse correlation of fluoride content of hydroxyl apatite with cell parameter is well known [30, 31]. In sample TiHAPF0.75, "a" parameter increases

again confirming the different behaviour in this samples which also seen in Raman analysis. Since the only difference of this sample with TiHAp is in fluoride content and contracting effect of fluoride on the hydroxyl apatite unit cell is well known it leads to conclusion that by adding the fluoride, titanium acts completely different. Position of titanium in apatite structure is a debate and there are some suggestions including the replacement in phosphorus or calcium positions [14, 32]. Comparing two Ca(I) and Ca(II) position by taking into account the total energy evaluation and structural optimisation Ti position led to predicting of existence of Ca(I) in hydroxyl apatite[33], but there isn't any theoretical study about the substitution of titanium in phosphorus position. However, considering the substitution of vanadium which has close ion radiation and electro negativity to titanium (ionic radius of titanium and vanadium are 0.6 and 0.59(A°), respectively) in phosphate position it is not so unlikely to consider phosphate place as a candidate to titanate group substitution. These explanations lead to assumption of titanium placed dominantly in phosphate or Ca(I) position in hydroxyl apatite structure. By adding fluoride it could be changed in these positions. However, clarification of the mechanism of this behaviour is hard to understand, but this situation is considered to be similar to uranium substitution in chlor apatite and fluor apatite which were studied by Luo et al. [34].

Uranium distributed almost equally between two Ca(I) and Ca(II) sites in chlor apatite, but in fluor apatite uranium partitions dominantly into Ca(II) site and also in this case the capacity of fluor apatite for uranium(2.09wt%) is higher than the one for fluor apatite(2.02wt%)[34]. The other possibility is changing the band length by adding fluoride in a way that more titanium could substituted in structure of fluoridated hydroxyl apatite without changing the position of it. In this case, the electronegative fluoride and Ca(II) atoms possess strong and shorter bond length and this will make the Ca(I) octahedron and phosphate locations more hospitable for titanium.

The results of zeta potential of the samples at pH=7.9 are shown in Figure 6. As it is seen in this figure, pure apatite structure has negative charge on the surface and by introducing titanium it become positive. Positive charge of the surface increases in TiHApF0.25 sample and it decreases again in TiHApF0.75.

In pure HAp anions such as HPO_4^{2-} and also unsatisfied oxygen ion charged [35] lead to negative charge of the surface. By adding titanium some part of the titanium ions adsorb on the surface. Since, not all of the titanium substituted in apatite structure and this situation will cause the existence of extra Ca^{2+} ions in the solution and adsorbing of Ca^{2+} , Ti^{4+} and other Ti containing cationic groups made the surface charge positive. On the other hand, substituted titanium changes the cell parameters

and also broadening and shifting of Raman peaks. In low concentration fluoride surface charge doesn't change significantly.

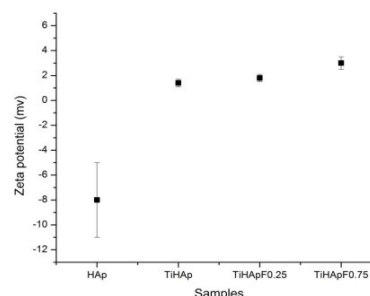


Figure 6. Zeta potentials of the samples at pH 7.9.

By increasing the fluoride amount in TiHApF0.75 the high electronegativity of fluoride might cause the affinity toward positively charged ions on the surface of the apatite, increasing the Ti concentration on the hydrated layer and increase the probability of the trapping of the Titanium ions by hydroxyl apatite during the maturation time and changing the position of the substituted titanium.

Figure 7. shows SEM micrographs of the different samples. It is obvious that neither titanium nor fluoride changed the morphology of the particles.

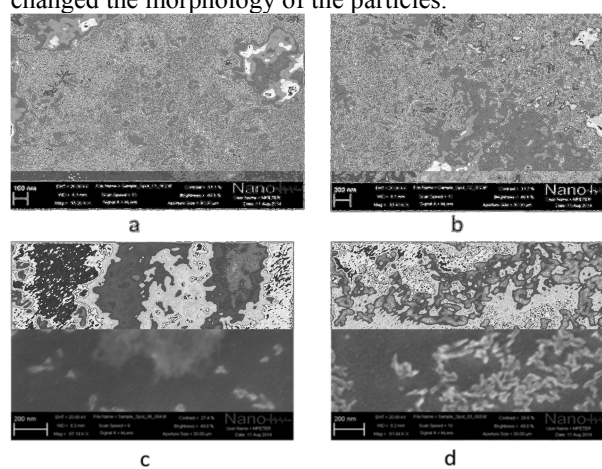


Figure 7. SEM images of the samples: a) HAp, b) TiHAp, c) TiHApF0.25, d) TiHApF0.75.

4. CONCLUSIONS

Titanium-containing hydroxyl apatite with two of concentrations of fluoride were synthesized and characterized. XRD, Raman and FTIR results showed that titanium incorporated to hydroxyl apatite structure. Calculating the cell parameters indicated the increasing of the cell parameter "a" by titanium introduction and decreasing of this parameter in TiHApF0.25 and increasing again in TiHApF0.75. Raman shift of the phosphate ν_1 peak in TiHApF0.75 also showed different changes from TiHApF0.25. Different position of the

titanium in the fluorohydroxy apatite and hydroxyl apatite could explain these results.

Zeta potential of pure apatite was negative while other three samples had positive surface charges. The morphology of hydroxyl apatite was not changed by adding Titanium and fluoride.

REFERENCES

- Rameshbabu, N., Kumar, T.S.S., Prabhakar, T.G., Sastry, V.S., Murty, K.V. and Rao, K.P., "Antibacterial nanosized silver substituted hydroxyapatite: synthesis and characterization", *Journal of Biomedical Materials Research*, Vol. 80, (2007), 581-591.
- Song, N., Liu, Y., Zhang, Y., Tan, Y.N. and grover, L.M., "Synthesis and characterisation of iron substituted apatite", *Advances in Applied Ceramics*, Vol. 111, No. 8, (2012), 466-471.
- Bigi, A., Boanini, E., Capuccini, C. and Gazzano, M., "Strontium-substituted hydroxyapatite nanocrystals", *Inorganica Chimica Acta*, Vol. 360, No. 3, (2007), 1009-1016.
- Feng, Z., Liao, Y. and Ye, M., "Synthesis and structure of Cerium substituted hydroxyapatite", *Journal of Materials Science: Materials in Medicine*, Vol. 16, (2005), No. 5, 417-421.
- Shpak, A.P., Karbovskii, V.L., Kurgan, N.A., Getman, E.I., Senkevich, A.I. and Marchenko, V.I., "Electron structure of apatite Like compounds with isomorph substitution in tetrahedral positions", *Functional Materials*, Vol. 12, (2005), 695-699.
- Ogo, S., Onda, A. and Yanagisawa, K., "Hydrothermal synthesis of vanadate-substituted hydroxyapatites, and catalytic properties for conversion of 2-propanol", *Applied Catalysis A: General*, Vol. 348, No. 1, (2008), 129-134.
- Karbovskii, V.L., Smolyak, S.S., Shpak, A.P., Zagorodniy, Y.A. and Kasaiyanenko, V.H., Electron structure of triple tetrahedral structures on the calcium hydroxyapatite basis, *Functional Materials*, Vol. 17,(2010), 151-157.
- Nakata, K., Kubo, T., Numako, C., Onoki, T. and Nakahira, A., "Synthesis and Characterization of Silicon-Doped Hydroxyapatite", *Materials Transactions*, Vol. 50, No. 5, (2009), 1046-1049.
- Vandiver, J., Dean, D., Patel, N., Botelho, C., Best, S., Santos, J.D., Lopes, M.A., Bonfield, W. and Ortiz, C., "Silicon addition to hydroxyapatite increases nanoscale electrostatic ", *Journal of Biomedical Materials Research*, Part A , Vol. 78, No. 2, (2006), 352-363.
- Alshemary, A.Z., Goh, Y.-F., Akram, M., Razali, I.R., Abdul Kadir, M.R. and Hussain, R., "Microwave Assisted Synthesis of Nano Sized Sulphate Doped Hydroxyapatite", *Materials Research Bulletin*, Vol. 48, No. 6, (2013), 2106-2110.
- Rehman, I. and Bonfield, W., "Characterization of hydroxyapatite and carbonated apatite by photo acoustic FTIR spectroscopy", *Journal of Materials Scienc: Materials in medicine*, Vol. 8, No. 1, (1997), 1-4.
- Wopenka, B., Pasteris, J.D., "A mineralogical perspective on the apatite in bone", *Materials Science and Engineering: C*, Vol. 25, No. 2, (2005), 131-143.
- Hu, A., Li, M., Chang, C., Mao, D., "Preparation and characterization of a titanium-substituted hydroxyapatite photocatalyst", *Journal of Molecular Catalysis A: Chemical*, Vol. 267, (2007), 79-85.
- Ergun, C., "Effect of Ti ion substitution on the structure of hydroxylapatite", *Journal of the European Ceramic Society*, Vol. 28, No. 11, (2008), 2137-2149.
- Kandori, K., Kuroda, T. and Wakamura, M., "Protein adsorption behaviors onto photocatalytic Ti(IV)-doped calcium hydroxyapatite particles", *Colloids and surfaces. B, Biointerfaces*, Vol. 87, (2011), 472-479.
- Slosarczyk, A., Zima, A., Paszkiewicz, Z., Szczepaniak, J., Aza, A.H. and Chrocicka, A., "The Influence of Titanium on Physicochemical Properties of Ti modified Hydroxyapatite Materials", *Materiały Ceramiczne /Ceramic Materials*, Vol. 62, (2010), 369-375.
- Nishikawa, M., Yang, W. and Nosaka, Y., "Grafting effects of Cu²⁺ on the photocatalytic activity of titanium-substituted hydroxyapatite", *Journal of Molecular Catalysis A: Chemical*, Vol. 378, (2013), 314-318.
- Sugiyama, S., Tanimoto, S., Fukuda, K., Kawashiro, K., Tomida, T. and Hayashi, H., "Immobilization of aqueous tetravalent cations of titanium and zirconium with calcium hydroxyapatite", *Colloids and Surfaces A: Physicochemical and Engineering Aspects*, Vol. 252, (2005), 187-192.
- Tanaka, H. and Ohnishi, A., "Synthesis of Ti(IV)-substituted calcium hydroxyapatite microparticles by hydrolysis of phenyl phosphates", *Advanced Powder Technology*, Vol. 24, No. 6, (2013), 1028-1033.
- Wakamura, M., Tanaka, H., Naganuma, Y., Yoshida, N. and Watanabe, T., "Surface structure and visible light photocatalytic activity of titanium-calcium hydroxyapatite modified with Cr(III)", *Advanced Powder Technology*, Vol. 22, No. 4, (2011), 498-503.
- Wakamura, M., Hashimoto, K. and Watanabe, T., "Photocatalysis by Calcium Hydroxyapatite Modified with Ti(IV): Albumin Decomposition and Bactericidal Effect", *Langmuir*, Vol. 19, No. 8, (2003), 3428-3431.
- Kandori, K., Oketani, M., Sakita, Y. and Wakamura, M., "FTIR studies on photocatalytic activity of Ti(IV)-doped calcium hydroxyapatite particles", *Journal of Molecular Catalysis A: Chemical*, Vol. 360, (2012), 54-60.
- Huang, J., Best, S.M., Bonfield, W. and Buckland, T., "Development and characterization of titanium-containing hydroxyapatite for medical applications", *Acta biomaterialia*, Vol. 6, No. 1, (2010), 241-249.
- Eslami, H., Solati-Hashjin, M. and Tahriri, M.R., "The comparison of powder characteristics and physicochemical, mechanical and biological properties between nanostructure ceramics of hydroxyapatite and fluoridated hydroxyapatite", *Materials Science and Engineering: C*, Vol. 29, No. 4, (2009), 1387-1398.
- Shahini, S., Askari, M. and Sadrmezhaad, S.K., "Gel-sol synthesis and aging effect on highly crystalline anatase nanopowder", *Bulleine of Materials Science*, Vol. 34, No. 6, (2011), 1189-1195.
- Wojdyr, M., "Fityk: a general-purpose peak fitting program", *Journal of Applied Crystallography*, Vol. 43, (2010), 1126-1128.
- Holland, T.J.B. and Redfern, S.A.T., "Unit cell refinement from powder diffraction data; the use of regression diagnostics", *Mineralogical Magazine*, Vol. 61, (1997), 65-77.
- Markovic, M., Fowler, B.O. and Tung, M.S., "Preparation and comprehensive characterization of a calcium hydroxyapatite reference material", *Journal of Research of the National Institute of Standards and Technology*, Vol. 109, (2004), 553-568.
- Campillo, M., Lacharaise, P.D., Reparaz, J.S., Goni, A.R. and Valiente, M., "On the assessment of hydroxyapatite fluoridation by means of Raman scattering", *The Journal of Chemical Physics*, Vol. 132, No. 24, (2010), 244501.
- Bianco, A., Cacciotti, I., Lombardi, M., Montanaro, L., Bemporad, E. and Sebastiani, M., "F-substituted hydroxyapatite

- nanopowders: Thermal stability, sintering behaviour and mechanical properties", *Ceramics International*, Vol. 36, No. 1, (2010), 313-322.
31. Okazaki, M., Miake, Y., Tohda, H., Yanagisawa, T. and Takahashi, J., "Fluoridated apatite synthesized using a multi-step fluoride supply system", *Journal of Biomaterials*, Vol. 20, No. 14, (1999), 1303-1307.
 32. Ribeiro, C.C., Gibson, I. and Barbosa, M.A., "The uptake of titanium ions by hydroxyapatite particles-structural changes and possible mechanisms", *Biomaterials*, Vol. 27, No. 9, (2006), 1749-1761.
 33. Tsukada, M., Wakamura, M., Yoshida, N. and Watanabe, T., "Band gap and photocatalytic properties of Ti-substituted hydroxyapatite: Comparison with anatase-TiO₂", *Journal of Molecular Catalysis A: Chemical*, Vol. 338, (2011), 18-23.
 34. Luo, Y., Hughes, J.M., Rakovan, J. and Pan, Y., "Site preference of U and Th in Cl, F, and Sr apatites", *American Mineralogist*, Vol. 94, (2009), 345-351.
 35. Lopes, M.A., Monteiro, F.J., Santos, J.D., Serro, A.P. and Saramago, B., "Hydrophobicity, surface tension, and zeta potential measurements of glass-reinforced hydroxyapatite composites", *Journal of Biomedical Materials Research*, Vol. 45, No. 4, (1999), 370-375.